Step-Scan Time-Resolved FTIR Spectroscopy of Cytochrome P-450$_{cam}$ Carbon Monoxide Complex: A Salt Link Involved in the Ligand-Rebinding Process†

Jörg Contzen and Christiane Jung*

Max Delbrück Center for Molecular Medicine Berlin-Buch, Robert-Rössle-Strasse 10, D-13122 Berlin, Germany

Received December 29, 1997; Revised Manuscript Received February 10, 1998

ABSTRACT: Step-scan time-resolved Fourier transform infrared spectroscopy with a time resolution of 5 μs was applied to the carbon monoxide complex of cytochrome P-450$_{cam}$ (CYP101) to study the bimolecular ligand-rebinding process after flash photolysis. Spectral changes in the CO ligand stretch vibration band and in the protein amide I′ band were monitored simultaneously. In substrate complexes having the camphor C-8, C-9, and C-10 methyl groups, rebinding of the ligand and the relaxation of the protein proceed at the same rate within experimental errors. For substrate complexes missing the methyl groups, the relaxation of the protein tends to relax slightly faster than the CO ligand rebinding to the heme iron. Compared to the (1*R*)-camphor and the camphane complex, the bimolecular rebinding rate constants for P-450 bound with substrates lacking the methyl groups are increased by a factor of 10−40. An unusual signal at about 1719 cm^{-1} was found in the difference spectrum of the photolyzed minus nonphotolyzed CO complex which has not been reported for other heme proteins so far. This signal is strongly pronounced in wild-type P-450$_{cam}$ bound with (1*R*)-camphor or camphane and in the D251N mutant bound with (1*R*)-camphor. In contrast, substrate-free P-450 and the norbornane and norcamphor complexes reveal only a very weak signal or a changed band shape. On the basis of the crystal structure data, we suggest that this signal originates from the rearrangement of the hydrogen-bonding pattern or the protonation state of the salt link between Asp297, Arg299, and the heme propionate group.

Cytochrome P-450$_{cam}$[1] (CYP101) is a member of the big CYP superfamily of cytochrome P-450 proteins (*1*) which are involved in several metabolic processes in animal and human organs, in fish, insects, plants, and bacteria (*2*). P-450s are unique in their ability to insert an oxygen atom from molecular oxygen into nonactivated carbon−hydrogen bonds. While interacting with molecular oxygen, these enzymes are also the source of cytotoxic reactive oxygen intermediates as, for example, hydrogen peroxide. There are indications that the accessibility of the enzyme structure for water molecules is an essential structural parameter for switching the cytochrome P-450 reaction cycle to the formation of hydrogen peroxide. Several experimental findings led to the supposition that the accessibility of the protein structure for water molecules is related to the mobility of the substrate bound in the heme pocket and to the flexibility of the protein structure itself (*3, 4*). To understand these relationships in terms of enzyme−substrate interaction and to set up methods to quantitate this dynamic behavior, we have investigated the bacterial cytochrome P-450$_{cam}$ in the substrate-free form and in the presence of various analogues of its natural substrate (1*R*)-camphor using different methods (*5*−*9*). It turned out that the CO stretch vibration mode measured by infrared spectroscopy is a valuable spectroscopic probe to characterize the active-site behavior when bound with different substrates. In particular, flash photolysis studies show that the rebinding kinetics of CO depend on the nature of the bound substrate and might be a good measure to quantitate the active-site dynamics (*5*).

Structural changes occurring in the cytochrome P-450 protein during photoinitiated reactions are commonly monitored by their influence on the heme electronic absorption bands (*10*−*16*). Unfortunately, changes of this spectroscopic probe cannot be assigned directly to distinct structural alterations within the protein. However, recent developments of modern step-scan Fourier transform infrared spectrometers allow the detection of time-dependent processes over a broad spectral range with a time resolution from milliseconds down to nanoseconds and sufficiently good signal-to-noise ratio, as have been demonstrated for hemoglobin and myoglobin to monitor changes of vibrational modes of the heme complex and of the protein (*17*−*19*). We applied this method for the first time to cytochrome P-450 to monitor the structural changes involved in the rebinding of photodissociated CO ligand in flash photolysis experiments. In the present paper, we will show that the bimolecular CO rebinding is connected with the relaxation of the whole protein and that a change in a salt link is involved in this process.

† This work was supported by the Deutsche Forschungsgemeinschaft (Grant Ju223/3-1 and SK35/3-1) and the European Community Biotechnology Program (Grant BIO2-CT94-2060).

* To whom correspondence should be addressed. Phone: 49-30-94063370. Fax: 49-30-94063329. E-mail: cjung@mdc-berlin.de.

[1] Abbreviations: FTIR, Fourier transform infrared; P-450$_{cam}$, cytochrome P-450 from *Pseudomonas putida* which catalyzes the hydroxylation of (1*R*)-camphor; CO, carbon monoxide; wt, wild-type protein of cytochrome P-450$_{cam}$; D251N, mutant of cytochrome P-450$_{cam}$ in which aspartate 251 was replaced by an asparagine residue; A_{280}, A_{391}, A_{417}, absorption at 280, 392, and 417 nm, respectively; UV−vis, ultraviolet−visible; dc, direct current; PTFE, polytetrafluoroethylen.

S0006-2960(97)03170-X CCC: $15.00
Published on Web 03/13/1998

MATERIALS AND METHODS

Protein Preparation. Wild-type cytochrome P-450$_{cam}$ from *Pseudomonas putida* was expressed in *Escherichia coli* strain TB1, isolated, and purified as described (*20*). Protein fractions with an absorption ratio A_{392}/A_{280} of at least 1.2 were selected for substrate removal by dialysis against 50 mM Tris-HCl buffer (pH 7.4, containing 5% glycerol by volume), followed by Sephadex G25 (medium) chromatography run in the same buffer. The substrate-free protein was reconcentrated by ultrafiltration using Centricon-30 (Amicon) and dialyzed against deuterated 100 mM potassium phosphate buffer (corresponding to pH 7.0) for 24 h to ensure complete H−D exchange. The final protein concentration was 1.38 mM with an absorbance ratio A_{417}/A_{280} of 1.49 (corresponding to A_{392}/A_{280} of 1.32) and was stored in small fractions at −70 °C until used for sample preparation.

The D251N mutant was a generous gift of C. Di Primo. It was expressed, isolated, and purified as previously described (*21*, *22*). For the H−D exchange, the 1.1 mM protein solution was diluted to the 34-fold volume with deuterated 100 mM potassium phosphate buffer (corresponding to pH 7.0) containing 400 μM (1*R*)-camphor to ensure complete substrate binding. After 24 h equilibration time, the protein solution was concentrated by means of Microcon-30 (Amicon) ultrafiltration tubes. To complete the H−D exchange, the protein solution was diluted with the same buffer to its 5-fold volume and reconcentrated by ultrafiltration for four times. The final protein concentration was 0.73 mM. Small fractions of the protein were stored at −70 °C until used for sample preparation. Cytochrome P-420 formation has not been observed after this procedure.

Preparation of the Carbon Monoxide Complex. (1*R*)-Camphor and the substrate analogues camphane, norcamphor, and norbornane were purchased from Aldrich or Sigma and were dissolved in ethanol-OD to give a 700 mM substrate solution. Equal volumes of protein solution and glycerol-d3 (Aldrich) were mixed to get 50% glycerol content by volume in order to stabilize the protein. Then, ethanolic substrate solution was added in 30-fold excess to get complete substrate binding. A strong gas stream of carbon monoxide from a steel cylinder passed over the surface of the sample solution for 1 min, then fresh prepared anaerobic 1 M sodium dithionite solution (in deuterated 100 mM potassium phosphate buffer) was added in 50-fold excess to reduce the sample. CO binding was completed by repassing carbon monoxide over the surface of the solution for 2 min. The sample was immediately filled in the IR sample cell, which consists of two CaF_2 windows separated by a 23 μm PTFE spacer. Sample preparation was also carried out with nondeuterated solvents in the same way, but with higher protein concentration. Sample cell path length was only 6 μm to reduce the water absorption in the amide I band. The sample quality was checked in the UV−vis spectrum, and the P-450$_{cam}$−CO concentration was determined by the absorption of the Soret band at 447 nm [absorption coefficent 121 mM^{-1} cm^{-1} (*21*)].

Description of the Spectrometer. Several publications deal with instrumental aspects of step-scan FTIR spectrometry (*23*, *24*). Infrared spectra were recorded on a Bruker IFS66 FTIR spectrometer with step-scan option for time-resolved FTIR spectroscopy. A photoconductive mercury cadmium telluride (MCT) detector with 1 μs rise time (D316 from Bruker) was used with a dc-coupled preamplifier. The output signal was digitized by the internal 16 bit analog-to-digital converter at a sampling rate of 200 kHz, allowing 5 μs time resolution. Antireflective germanium long wave pass filters with cut-on frequencies at 5882 and 2605 cm^{-1} in the IR beam limited the spectral bandwidth and protected interferometer and detector from scattered radiation of the photolysis laser. The whole instrument stands on a vibration isolation table to decouple it from vibrations of the building. The stability of the interferometer mirror was measured by means of the reference HeNe laser signal. When held at a fixed position, the signal variation was about ±118 mV, compared to ±4.88 V peak amplitude during positioning. From these values, we calculated the positional error to be within ±2.4 nm for our instrument.

The frequency doubled output at 532 nm of a Q-switched Nd:YAG laser (Surelite I from Continuum) served as light source for flash photolysis. The output energy of the laser was typically 2.2 mJ/pulse with 4−6 ns pulse width at a beam diameter of 6 mm measured at the sample position. A trigger pulse from the spectrometer started data acquisition and fired the flash lamp of the laser. After an internal delay of 200 μs, the Q-switch was toggled and lasing took place. Starting data collection before lasing allowed a number of reference points to be collected. The reaction in the sample had completely relaxed after 100 ms, so the flash photolysis experiment can be repeated at a rate of 10 Hz to match the repetition rate of the laser.

Flash Photolysis Experiments. For each step-scan run, 1332 single-sided interferogram points were recorded to get 4 cm^{-1} spectral resolution at 5 or 40 μs time resolution. Up to 500 time slices were stored to give a maximum observation time of 20 ms. The settling time for the interferometer mirror was set to 100 ms. At each interferogram point, the signal from 48 sample excitations was averaged to increase the signal-to-noise ratio. Blackman-Harries 3-term apodization with 32 cm^{-1} phase resolution and the Mertz phase correction algorithm was applied to each interferogram prior to Fourier transformation with a zero-filling factor of 4. From the resulting single channel spectra, the time range from 0 to 200 μs was averaged to get a dark-intensity-spectrum I_D of the undisturbed sample. Absorbance difference spectra were calculated from the single channel spectra as $\Delta\mathrm{Abs}(t) = -\log[I(t)/I_D]$. Absorbance difference spectra from at least five step-scan runs were finally averaged to yield a sufficiently good signal-to-noise ratio.

The fraction of photolyzed P-450−CO complex is calculated from the ratio of the CO stretch bands integrated absorbance at time zero of the difference spectrum to the integrated absorbance of the static spectrum.

A test experiment was run with hen egg albumin, which undergoes no photoinitiated reaction, to ensure, that neither radio frequency noise emitted from the laser nor that scattered laser light affected the detector or components of the spectrometer electronics. All experiments were made at a sample temperature of 27 °C. Integrity of the P-450$_{cam}$−CO complex was checked by UV−vis spectrometry before and after flash photolysis experiments.

Fitting the Experimental Time Course. A simple one-state model [P-450 + CO → P-450−CO] was assumed to fit the kinetic data to second-order reaction kinetics for the rebind-

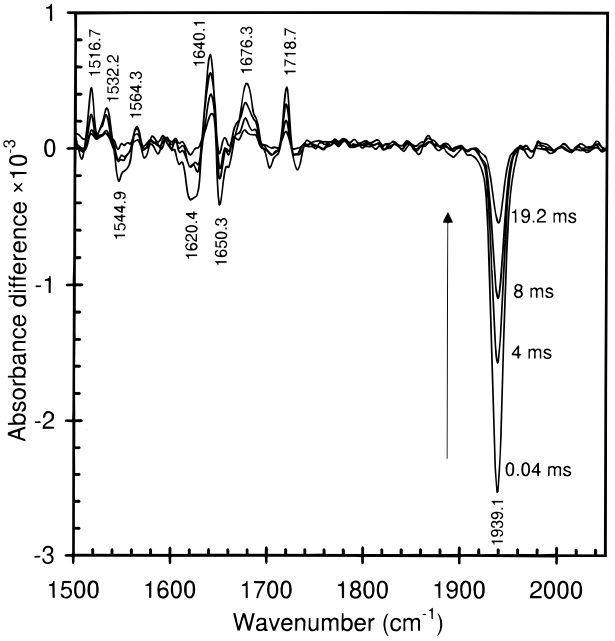

FIGURE 1: Time-resolved absorption difference spectra of wild-type cytochrome P-450$_{cam}$−CO complex with (1*R*)-camphor substrate. Spectra at 0.04 and 4 ms are the average of 5, those at 8, 12, and 19.2 ms are the average of 10 time slices to reduce the noise.

ing of carbon monoxide to cytochrome P-450, neglecting the thermal dissociation of the carbon monoxide complex. Integration of the appropriate differential equation leads to an expression for the absorbance difference between the photolyzed and the nonphotolyzed sample, which was fitted to the experimental data using a nonlinear least-squares method:

$$\Delta\mathrm{Abs}(t) = \epsilon l\left([\mathrm{P450}]_0\frac{\exp[k_{on}t([\mathrm{CO}]_0-[\mathrm{P450}]_0)]-1}{\exp(k_{on}t[[\mathrm{CO}]_0-[\mathrm{P450}]_0)]-\dfrac{[\mathrm{P450}]_0}{[\mathrm{CO}]_0}}-[\mathrm{P450CO}]_\infty\right) \quad (1)$$

where $[\mathrm{P450}]_0$ and $[\mathrm{CO}]_0$ are the initial P-450 and carbon monoxide concentrations, respectively, generated by the laser flash, and $[\mathrm{P450CO}]_\infty$ is the concentration of the carbon monoxide complex in the dark sample. ϵ is the wavenumber dependent molar absorption coefficient or the integral molar absorption coefficient, l the thickness of the sample, and k_{on} the second-order rebinding constant. The initial P-450 concentration is calculated from total P-450-CO concentration determined from the Soret absorption and multiplied by the fraction of the photolyzed sample monitored immediately after the laser flash. The initial CO concentration was set to the initial P-450 concentration plus 0.8 mM, the solubility of CO in phosphate buffer (*25*). For stable fitting results, the initial concentrations have been held constant, and ϵl and k_{on} have been varied.

RESULTS

Time-resolved difference infrared spectra of cytochrome P-450$_{cam}$ bound with (1*R*)-camphor are shown in Figure 1.

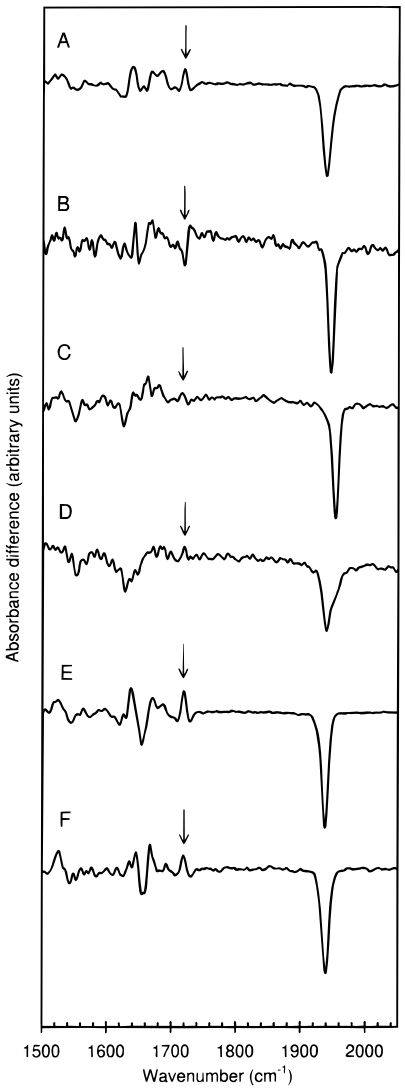

FIGURE 2: Absorption difference spectra of cytochrome P-450$_{cam}$−CO complex with (A) camphane (wt, D_2O), (B) norcamphor (wt, D_2O), (C) norbornane (wt, D_2O), (D) substrate free (wt, D_2O), (E) (1*R*)-camphor (D251N mutant, D_2O), (F) (1*R*)-camphor (wt, H_2O) just after the laser flash. The first 50 time slices were averaged for clear resolution of the small absorption changes in the amide I′ band, except for spectrum D, where only 20 spectra could be averaged. Spectra were normalized to unity CO band area. The CO peak absorptions are (A) −1.74 m o.d., (B) −0.45 m o.d., (C) −0.69 m o.d., (D) −0.24 m o.d., (E) −2.72 m o.d., (F) −1.35 m o.d. Arrows indicate the peaks originating from the salt link as discussed in the text.

The first spectrum available at 40 μs after the laser flash shows completely developed bands, which decay with progress in time. The most intense negative band at 1939 cm^{-1} arises from the stretch vibration of the heme-bound CO, which is dissociated from the heme iron due to the laser flash (*5*, *20*). Bands between 1690 and 1610 cm^{-1} are located in the amide I′ region and originate from the C═O stretch vibrations of the amide groups coupled to in-plane N−D bending and C−N stretching modes (*26*−*29*). Therefore, the positive peak at 1676 cm^{-1} indicates an increase of turn structure and the negative peak at 1650 cm^{-1} indicates a decrease of α-helix content due to CO dissociation. The assignment of the positive peak at 1640 cm^{-1} is ambiguous, because it could be related to increasing unordered structures, but also to α-helical or 3_{10}-helical components. The negative

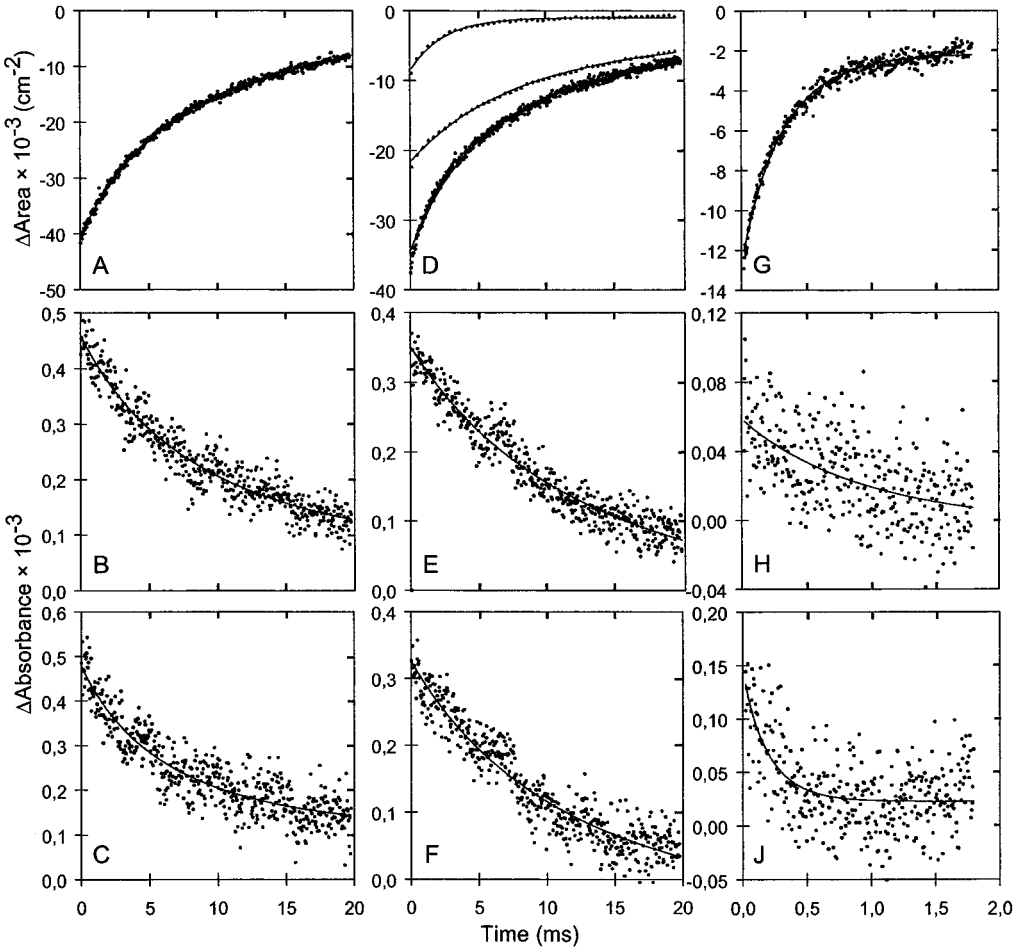

FIGURE 3: Carbon monoxide rebinding as monitored by the integrated area of the CO stretch vibration, and changes in the amide-I′ band induced by the transition from the unligated to the ligated state in wt cytochrome P-450$_{cam}$. (A−C) (1*R*)-camphor, (A) CO band area, (B) salt link at 1718.7 cm^{-1}, (C) turns at 1676.3 cm^{-1}; (D−F) camphane, (D) (●) total CO band area (low trace), (▲) substate at 1939.3 cm^{-1} (middle trace), (◆) substate at 1949.2 cm^{-1} (upper trace), (E) salt link at 1718.8 cm^{-1}, (F) turns at 1684.6 cm^{-1}; (G−J) norbornane, (G) CO band area, (H) salt link at 1715.5 cm^{-1}, (J) turns at 1680.3 cm^{-1}.

peak at 1620 cm^{-1} corresponds to decreasing β-sheet content (*29*).

The bands between 1564 and 1516 cm^{-1} lie in the range of the amide II band, which arise from N−H bending vibrations of the peptide backbone. Due to incomplete H−D exchange of strongly bound hydrogens, the amide II band has not shifted completely to the 100 cm^{-1} lower located amide II′ band, hence it might interfere with signals from amino acid side chains, especially from COO$^-$ groups (*30*, *31*).

The positive peak at 1719 cm^{-1} can be assigned to the C═O stretch vibration of a COOH group. Aspartic acid or glutamic acid residues but also the heme propionic acid group are possible candidates which become protonated when the CO iron ligand is dissociated. The other possible assignment to the keto group of the camphor substrate, showing the CO stretch band at 1720 cm^{-1} in D_2O buffer, can be ruled out because the peak is still present in camphane-bound P-450$_{cam}$, which lacks this keto group, as shown in Figure 4A.

To test the influence of the substrate structure on the protein relaxation after CO dissociation, different substrate analogue P-450$_{cam}$−CO complexes have been measured. Transient difference spectra recorded immediately after CO dissociation are shown in Figure 2. Common to all substrate−P-450 complexes under investigation are one or two peaks between 1663 and 1688 cm^{-1}, indicating an increase of turn structure. For camphane-bound wt P-450, a signal in the region of 1650 cm^{-1} is absent, indicating no change in α-helical structure due to CO dissociation. If norcamphor is used as substrate, the CO stretch vibration of the heme-bound CO shifts to higher wavenumber (1946.1 cm^{-1}), in agreement with the band position of the static absorption spectrum of the CO complex (*7*, *20*). Below 1660 cm^{-1}, the difference spectrum suffers on increasing noise, so no further signals were resolved. Assuming that the negative peak at 1719.6 cm^{-1} originates from the stretch vibration of a COOH group, like in camphor-bound and camphane-bound P-450, then a deprotonation of the COOH group induced by the dissociation of the CO ligand would be expected because of the negative sign of this signal. This behavior is inverse to that seen for the camphor complex. Furthermore, the signal shows stronger wings indicating more a shift of this band during the photolysis than the appearance of a new band. In contrast, P-450 bound with norbornane has only a very weak signal at 1715.5 cm^{-1}. In the amide I′ region, the negative peak at 1624.8 cm^{-1} allows the assumption of decreasing β-sheet content in this substrate complex. The stretch vibration of the iron CO ligand is shifted to higher wavenumbers (1953.1 cm^{-1}) compared to camphor-bound P-450.

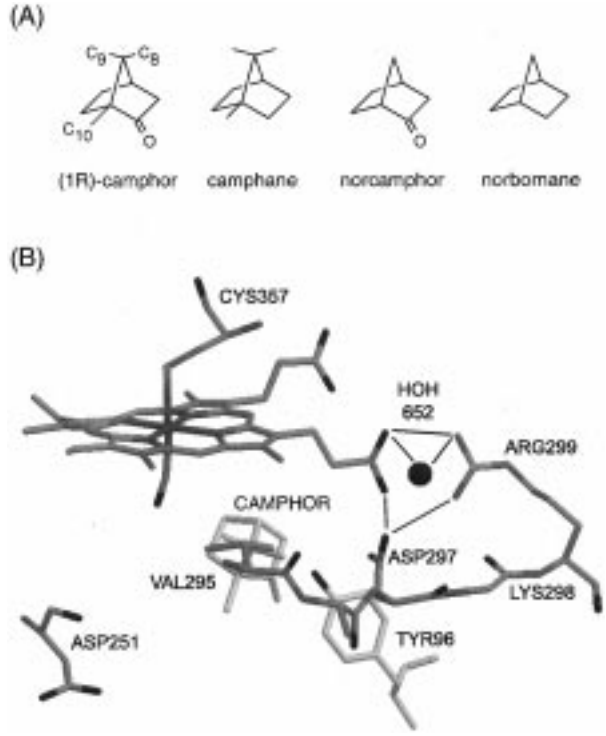

FIGURE 4: (A) Compound structure and numbering sequence for methyl groups of substrate analogues used in the experiments. (B) View on the active site of P-450$_{cam}$ with the proposed salt link between the heme propionate group, Asp297 and Arg299. From the crystal structure of the ternary P-450$_{cam}$−CO (1*R*)-camphor complex (*35*) (PDB file 3CPP).

Substrate-free P-450$_{cam}$ has a broad heme CO band peaked at 1939.8 cm^{-1} which results from an overlap of several subbands (*6*). The COOH group signal is also very weak but still detectable at 1719.6 cm^{-1}. All signals are of very low intensity compared to camphor-bound or camphane-bound P-450.

For the camphor-bound D251N mutant P-450, the difference spectrum (Figure 2E) is similar to that of the wt P-450, but the intensity of the negative peak at 1654.2 cm^{-1} in the α-helical region is of higher intensity. This would probably mean that more α-helical structure is converted to other structure elements than in the wt protein, also reflecting the lower stability of the D251N mutant (*32*).

The peptide C═O stretch vibrations in the amide I′ band are influenced only weakly by isotopic effects of the solvent because the hydrogen bonds within the secondary structures are relatively stable and this stretch vibration couples only weakly with the peptide N−H bending mode. Only slight band shifts to lower wavenumbers are usually observed when H_2O is replaced by D_2O (*26*). Our comparative experiments for camphor-wt-P-450 measured in D_2O and H_2O buffer (Figure 1 and Figure 2F) are in agreement with this general observation. There is essentially no shift in the peak positions of the difference spectrum in the amide I band (H_2O) compared to the amide I′ band (D_2O). The signal at 1719 cm^{-1} also does not show an isotopic shift.

All well-resolved positive and negative peaks in the light minus dark difference spectrum have been checked concerning their time traces. Most of them follow a clear relaxation kinetics analogously to the kinetics seen in the CO ligand stretch mode band. Table 1 summarizes the bimolecular rate constants k_{on} which have been obtained from fitting the time-dependent absorbance changes using eq 1. Figure 3 shows selected representative time traces with their corresponding fit curves as examples to demonstrate the experimental accuracy and fit quality. Because the CO ligand infrared spectrum shows subbands for some complexes (camphane, substrate-free) the time-dependent integrated absorbance (total area) was used for fitting the time traces monitored in the CO ligand bands. k_{on} values for the CO ligand substates in camphane complex and in substrate-free P-450 have been obtained from the fit of the time-dependent absorbance of the single subbands after a curve fitting with gaussians.

In substrate complexes having the camphor C-8, C-9, and C-10 methyl groups (see Figure 4A), the rebinding of the ligand and the relaxation of the protein proceed at the same rate within experimental errors. For substrate complexes missing the methyl groups, the proteins tend to relax slightly faster than the CO rebinding to the heme iron. Compared to the (1*R*)-camphor and the camphane complex, the bimolecular rebinding rate constants for P-450 bound with substrates lacking the methyl groups are increased by a factor of 10−40.

DISCUSSION

(i) Assignment of the 1719 cm^{-1} Signal. As already mentioned, the positive peak at 1719 cm^{-1} must be assigned to the C═O stretch vibration of a COOH group of an aspartic or glutamic acid side chain or the heme propionic acid group. For the free amino acids, the CO stretch vibration is observed at 1716 cm^{-1} (H_2O) and 1713 cm^{-1} (D_2O) for Asp ($C_\beta OOH$), respectively, at 1712 and 1706 cm^{-1} for Glu ($C_\gamma OOH$). In the deprotonated form, the asymmetric vibration of COO^- is found at 1574 cm^{-1} (H_2O) and 1584 cm^{-1} (D_2O) for Asp and at 1560 cm^{-1} (H_2O) and 1567 cm^{-1} (D_2O) for Glu (*30*, *31*). Similarily, the propionic acid group of protoporphyrin IX shows the infrared bands at 1740 cm^{-1} for the protonated state and at 1580 cm^{-1} for the deprotonated state as antisymmetric vibration and at 1390 cm^{-1} as symmetric vibration (*33*). Hydrogen bonding of an arginine, lysine, or histidine to the CO group of a COOH residue, as commonly observed in salt links, might modify the CO stretch vibration frequency between 1700 and 1740 cm^{-1}. This has been extensively studied for bacteriorhodopsin (*34*). So, we assign the peak at 1719 cm^{-1} as representative of a salt link. The effect of the substrates and the insensitivity against the H/D-exchange and against the mutation D251N on this band allow a clear assignment to a distinct salt link in the protein core near the substrate-binding region. Photoacoustic experiments suggest that the Arg186-Asp251-Lys178 bifurcated salt bridge is desolvated by flash photolysis of the CO complex (*32*). Replacing Asp251 by Asn should disturb the salt bridge, and the infrared band at 1719 cm^{-1} should disappear or at least be affected. No effects on the band are observed by the mutation (Figure 2E), so we exclude the region around Asp251 as origin for the 1719 cm^{-1} peak. In contrast, the substrate methyl groups have a clear influence on this band. If the methyl groups are removed from the substrate, the band changes its shape and sign (norcamphor) or is very weak (norbornane). From the crystal structure, one can see that there are hydrophobic contacts of the camphor methyl groups C-8 and C-9 to Val295 and Asp297 (*35*). Asp297 is involved in the salt link between Arg299 and the heme

Table 1: Bimolecular Rebinding Rate Constants Obtained from Nonlinear Least-Squares Fitting of the Experimental Data at 300 K[a]

substrate, protein, and solvent	[P-450-CO] (mM)	fraction[b] photolyzed	ϵ_{CO}[c] (10^4 M^{-1} cm^{-2})	k_{on} (10^4 $M^{-1}s^{-1}$) CO ligand	salt link	turns	α-helix	β-sheet
(1*R*)-camphor wt, D_2O	0.787	0.84	2.42 ± 0.01	9.8 ± 0.1 (1939.1)	8.6 ± 0.6 (1718.7; 8)[e]	11.9 ± 1.0 (1676.3)	7.4 ± 1.5 (1650.3); 8.5 ± 1.0 (1640.1)	14.5 ± 1.5 (1620.4)
camphane wt, D_2O	0.939	0.71	1.88 ± 0.01	12.4 ± 0.2 (1939.2) substates: 10.4 ± 0.3 (1939.4; 61)[d] 49.7 ± 1.8 (1949.2; 25)[d]	5.8 ± 0.4 (1718.8; 7)[e]	6.3 ± 0.5 (1684.6); 5.1 ± 1.0 (1668.3)	9.7 ± 1.2 (1638.5)	34.5 ± 3.0 (1623.1)
norcamphor wt, D_2O	0.776	0.14	2.59 ± 0.03	340.8 ± 7 (1946.1)	406.3 ± 55 (1719.6;−8)[e]	474.4 ± 76 (1668.7)		
norbornane wt, D_2O	0.877	0.18	2.91 ± 0.03	343.5 ± 6 (1953.3)	109.0 ± 41 (1715.5, 4)[e]	562.5 ± 85 (1680.3); 371.5 ± 85 (1663.1)		648.8 ± 135 (1624.8)
substrate free wt, D_2O	0.823	0.15	1.79 ± 0.03	190.2 ± 5 (1939.8) substates: 158.1 ± 11 (1941.2; 54)[d] 132.5 ± 13 (1951.9; 8)[d] 381.3 ± 29 (1960.1; 31)[d]	235.9 ± 86 (1719.6; 4)[e]	271.6 ± 55 (1681.8)		
(1*R*)-camphor wt, H_2O	3.096	0.86	2.29 ± 0.01	21.3 ± 0.3 (1939.5)	25.5 ± 2.2 (1719.1;10)[e]	34.2 ± 6.8 (1667.1)	19.1 ± 6.1 (1654.9)	
(1*R*)-camphor D251N, D_2O	1.182	0.62	2.36 ± 0.01	10.3 ± 0.1 (1938.2)	8.7 ± 0.4 (1719.6; 7)[e]	12.6 ± 1.6 (1687.5) 15.3 ± 1.6 (1670.8)	5.1 ± 1.5 (1654.2)	10.4 ± 1.6 (1637.5)

[a] Values in parenthesis indicate maximum peak wavenumber in cm^{-1}. [b] From the ratio of the area of the CO ligand infrared band directly after flash to the area of the dark spectrum. [c] Integral absorption coefficient. [d] Values in parentheses indicate the band maximum position and the percentage population of this band in the case of substates. [e] Values in parentheses indicate the band maximum position and the percentage ratio of the salt link band area to the total area of the CO ligand bands.

propionic acid group. So, the salt link between Asp297, Arg299, and the heme propionate group (Figure 4B) seems to be the best candidate for the origin of the 1719 cm^{-1} peak. This salt link is also not too strong (*36*) so that structural changes induced by the photodissociation of the CO ligand can affect the protonation equilibrium. All other aspartic or glutamatic acid groups and the other propionic acid group of the heme are too distant to be influenced by the substrate. Oprea et al. (*37*) suggest that Arg299 in the salt link with Asp297 and the propionate at the A pyrrol ring of the heme might change from an initial, stable side-chain conformation to another rotamer which forms a functional water channel from the active site to a water cluster located on the thiolate side of the heme, close to the protein surface. One should expect an effect of the H_2O/D_2O exchange on the 1719 cm^{-1} peak which is however not observed. Whether this contradicts our assignment or the model of Oprea et al. cannot be decided at present. The appearance of the salt link peak at 1719 cm^{-1} seems to be unique for P-450. Time-resolved FTIR experiments on myoglobin (*18*) and hemoglobin (*19*) do not report signals in the salt link region (1700−1740 cm^{-1}). However, photoacoustic calorimetry suggests intermediate opening of the Arg45-heme propionate salt link in myoglobin (*38*) and of the Arg186-Asp251-Lys178 salt link in P-450_{cam} (*32*) on the nanosecond time scale.

(ii) Substrate Modulated Rebinding Dynamics of the Active Site and the Protein. Biomolecular rebinding constants k_{on} for P-450_{cam} bound with various substrates have been determined by several groups from flashphotolysis studies using the heme electronic absorption band (Soret band) as probe (*11, 14*). Recently, a comparative (Soret band) flashphotolysis study of three different P-450 proteins in the absence and presence of their natural substrates has been reported for the time window of nanoseconds to 1 s and the temperature range of 78−297 K (*16*). Under these experimental conditions, the geminate recombination of the CO ligand can also been analyzed which is not possible to do with our time resolution of 5 μs and the temperature of 300 K. The bimolecular rate constant for the camphor-bound P-450cam in Table 1 determined from the integrated absorbance change in the CO ligand stretch infrared band is in excellent agreement with the rate constant obtained with the Soret band (*11, 14, 16*). With both signals (the CO stretch infrared bands and the heme Soret band), only the heme environment is probed. With the step-scan FTIR technique, we are now able to probe changes in the secondary structure and in the salt link during rebinding.

In substrate complexes having the camphor C-8, C-9, and C-10 methyl groups, the k_{on} rate constants determined at the signals for the secondary structure, for the CO ligand and at the 1719 cm^{-1} peak, are equal within the error of the experiments and the fitting procedure. For substrate complexes missing the methyl groups, the protein tends to relax slightly faster than the CO ligand during the rebinding to the heme iron (factor 1.5−2.0). However, because the signals for these complexes are rather small and the signal-to-noise ratio and therefore the mean error of the k_{on} values are not so good compared to the spectra of the methyl-containing substrate complexes, we would not overestimate this slightly faster relaxation of the protein signals. In particular, the errors for k_{on} determined from the salt link peak for the norbornane, and the substrate-free complexes are rather high although the data of 10 experiments have been averaged. So, we hesitate to interpret the quantitative

difference to the k_{on} values obtained from the other signals in these both complexes. Summarizing all complexes, we conclude that the protein and the salt link have a relaxation kinetics in the same order as the CO iron ligand. A more detailed analysis is required for the camphane and the substrate-free complexes, which both show at least two conformational substates for the CO iron ligand with comparable population which have different rebinding kinetics (Table 1) (*6*, *20*). This explains the slightly systematic deviation of the fit curve from the experimental time trace for the integrated absorbance of the CO ligand bound to this P-450 complex (Figure 3D). The k_{on} values for these substates given in Table 1 were obtained with the simple fit model presented in Materials and Methods where interconversion between the substates during rebinding has been neglected. Whether in the camphane complex, the faster rebinding of substate 2 [ν(CO) at 1949.2 cm^{-1}] can be assigned to the faster relaxation of the β-sheet signal and the slower rebinding of substate 1 [ν(CO) at 1939.4 cm^{-1}] to the slower relaxation of the turns remains still an open question and will be discussed elsewhere.

Great differences between the k_{on} rebinding constants have been observed when comparing the different P-450 substrate complexes. The fastest rebinding with a 30−40-fold increase of k_{on} compared to (1*R*)-camphor P-450 is observed for norcamphor and norbornane complexes, both missing the methyl groups (see Figure 4A). This faster rebinding seems to reflect the higher mobility of the substrate and the more flexible protein structure which have been already discussed in earlier papers (*3*, *4*, *14*, *39*). Substrate-free P-450 shows a 20-fold faster rebinding compared to camphor-bound P-450. For these three complexes, the salt link signal differs from the other complexes: it is rather small or has an inverse sign indicating that rebinding kinetics and salt link behavior might be correlated. The strongly increased rebinding rate constant for these three complexes obtained by our infrared measurements is qualitatively in agreement with the data from the Soret band flashphotolysis studies (*11*, *14*, *16*). However quantitatively, the infrared studies reveal only a 20−40-fold increase compared to the 80−100-fold increase obtained at the Soret band (*11*, *14*, *16*). Further experiments under comparable conditions such as glycerol content and protein concentration and using the Soret band as well as the CO stretch band as spectroscopic probes are required to clarify this quantitative difference.

In contrast, the D251N mutant with (1*R*)-camphor as substrate reveals the same rebinding rate as the wild-type protein. Interestingly, the rebinding rate in (1*R*)-camphor wt P-450 is increased by a factor of 2.2 in H_2O buffer compared to D_2O buffer which might reflect the general higher structural stability observed in the presence of D_2O (*29*).

From the presented data, we conclude that time-resolved step-scan FTIR spectroscopy allows detection of small conformational changes connected with an alteration of the protonation equilibrium of COOH groups in the salt link Asp297, Arg299, and the heme propionate group and in the secondary structure induced by CO binding which can hardly be seen in the crystal structure. This alteration is modulated by the nature of the substrate bound in the heme pocket. For cytochrome $P\text{-}450_{cam}$, it now seems to be clear that the methyl groups of the camphor molecule and their contacts to the protein are the most important structural elements which influence the bimolecular rebinding rate of the photodissociated CO ligand.

ACKNOWLEDGMENT

We thank Carmelo Di Primo (Institut de Biologie Physico-Chimique, INSERM-INRA U310, Paris) for generously donating the D251N mutant protein. Friedrich Siebert, Christoph Rödig (Albert-Ludwig-Universität, Freiburg), and Wilfried Hartmann (Bruker-Saxonia, Leipzig) are gratefully acknowledged for their help with the step-scan technique.

REFERENCES

1. Nelson, D. R., Koymans, L., Kamataki, T., Stegeman, J. J., Feyereisen, R., Waxman, D. J., Waterman, M. R., Gotoh, O., Coon, M. J., Estabrook, R. W., Gunsalus, I. C., and Nebert, D. W. (1996) *Pharmacogenetics* 6, 1−42.
2. Lewis, D. F. V. (1996) *Cytochromes P-450: Structure, Function and Mechanism*, Taylor & Francis Ltd, London.
3. Fisher, M. T., and Sligar, S. G. (1987) *Biochemistry 26*, 4797−4803.
4. Schulze, H., Hui Bon Hoa, G., and Jung, C. (1997) *Biochim. Biophys. Acta 1338*, 77−92.
5. Contzen, J., Ristau, O., and Jung, C. (1996) *FEBS Lett. 383*, 13−17.
6. Jung, C., Ristau, O., Schulze, H., and Sligar, S. G. (1996) *Eur. J. Biochemistry 235*, 660−669.
7. Jung, C., Schulze, H., and Deprez, E. (1996) *Biochemistry 35*, 15088−15094.
8. Schulze, H., Hui Bon Hoa, G., Helms, H., Wade, R., and Jung, C. (1996) *Biochemistry 35*, 14127−14138.
9. Mouro, C., Bondon, A., Simonneaux, G., and Jung, C. (1997) *FEBS Lett. 414*, 203−208.
10. Shiro, Y., Kato, M., Iizuka, T., Nakahara, K., and Shoun, H. (1994) *Biochemistry 33*, 8673−8677.
11. Kato, M., Makino, R., and Iizuka, T. (1995) *Biochim. Biophys. Acta 1246*, 178−184.
12. Koley, A. P., Buters, J. T. M., Robinson, R. C., Markowitz, A., and Friedman F. K. (1995) *J. Biol. Chem. 270*, 5014−5018.
13. Koley, A. P., Robinson, R. C., and Friedman, F. K. (1996) *Biochimie 78*, 706−713.
14. Unno M., Ishimori, K., Ishimura, Y., and Mosishima, I. (1994) *Biochemistry 33*, 9762−9768.
15. McLean, M. A., Yeom, H., and Sligar, S. G. (1996) *Biochimie 78*, 700−705.
16. Tétreau, C., Di Primo, C., Lange, R., Tourbez, H., and Lavalette, D. (1997) *Biochemistry 36*, 10262−10275.
17. Palmer, R., Chao, J. L., Dittmar, R. A., Gregoriou, V., and Plunkett, S. E. (1993) *Appl. Spectrosc. 47*, 1297−1310.
18. Plunkett, S. E., Chao, J. L., Tague, T. J., and Palmer, R. A. (1995) *Appl. Spectrosc. 49*, 702−708.
19. Hu, X., Frei, H., and Spiro, T. G. (1996) *Biochemistry 35*, 13001−13005.
20. Jung, C., Hui Bon Hoa, G., Schröder, K.-L., Simon, M., and Doucet, J. P. (1992) *Biochemistry 31*, 12855−12862.
21. Gunsalus, I. C., and Wagener, G. C. (1978) *Methods Enzymol. 52*, 116−188.
22. Gerber, N. C. (1993) Ph.D. Thesis, University of Illinois, Urbana, IL.
23. Manning, C. J., Chao, J. L., and Palmer, R. A. (1991) *Rev. Sci. Instrum. 62*, 1219−1229.
24. Uhmann, W., Becker, A., Taran, C., and Siebert, F. (1991) *Appl. Spectrosc. 45*, 390−397.
25. McKinnie, R., and Olson, J. S. (1981) *J. Biol. Chem. 256*, 8928−8932.
26. Surewicz, W. K., and Mantsch, H. H. (1988) *Biochim. Biophs. Acta 952*, 115−130.

27. Susi, H., and Byler, D. M. (1988) *Methods Enzymol. 130*, 290−311.
28. Byler, D. M., and Susi, H. (1986) *Biopolymers 25*, 469−487.
29. Mouro, C., Jung, C., Bondon, A., and Simonneaux, G. (1997) *Biochemistry 36*, 8125−8134.
30. Chirgadze, Yu. N., Fedorov, O. V., and Trushina, N. P. (1975) *Biopolymers 14*, 679−694.
31. Venyaminov, S. Yu., and Kalnin, N. N. (1990) *Biopolymers 30*, 1243−1257.
32. Di Primo, C., Deprez, E., Sligar, S. G., and Hui Bon Hoa, G. (1997) *Biochemistry 36*, 112−118.
33. Spiro, T. G. (1983) in *Physical Bioinorganic Chemistry Series: Iron Porphyrins, Part III* (Lever, A. B. P., and Gray, H. B., Eds.) pp 89−159, Addison-Wesley, London.
34. Bousché, O., Sonar, S., Krebs, M. P., Khorana, H. G., and Rothschild, K. J. (1992) *Photochem. Photobiol. 56*, 1085−1095.
35. Poulos, T. L., Finzel, B. C., and Howard, A. J. (1987) *J. Mol. Biol. 195*, 687−700.
36. Lounnas, V., and Wade, R. (1997) *Biochemistry 36*, 5402−5417.
37. Oprea, T. I., Hummer, G., and Garcia, A. E. (1997) *Proc. Natl. Acad. Sci. U.S.A. 94*, 2133−2138.
38. Westrick, J. A., Peters, K. S., Ropp, J. D., and Sligar, S. G. (1990) *Biochemistry 29*, 6741−6746.
39. Raag, R., and Poulos, T. L. (1991) *Biochemistry 30*, 2674−2684.

BI9731706